JOURNAL OF CATALYSIS 157, 97–108 (1995)

Modification of the Activity of $Mg_3(PO_4)_2$ in the Gas-Phase Conversion of Cyclohexanol by Addition of Sodium Carbonate

M. A. Aramendía,* V. Borau,* C. Jiménez,*,[1] J. M. Marinas,* F. J. Romero,* J. A. Navío,† and J. Barrios‡

Departamentos de Química Orgánica, and ‡Química Inorgánica, Facultad de Ciencias, Universidad de Córdoba, Avda. San Alberto Magno s/n, E-14004 Córdoba, Spain; and †Instituto de Ciencia de los Materiales, Universidad de Sevilla-CSIC/Departamento de Química Inorgánica, Facultad de Química, Avda. Reina Mercedes, E-41012 Sevilla, Spain*

Received October 19, 1994; revised March 20, 1995; accepted June 12, 1995

This paper reports the synthesis and characterization of solid $NaMgPO_4$, obtained by adding Na_2CO_3 to freshly formed $Mg_3(PO_4)_2 \cdot 22H_2O$. The magnesium orthophosphate was prepared by gelling an aqueous solution of $MgCl_2$ and Na_2HPO_4 with 3 *N* NaOH. The solid products thus obtained were characterized by using various structural (XRD), surface (XPS, DRIFT, BET), and morphological (SEM) elucidation techniques. The results show that the $NaMgPO_4$ surface also contains Na_2CO_3, NaCl, and MgO, which endow it with increased activity and selectivity. Thus, $Mg_3(PO_4)_2$ yields cyclohexene (CHE) preferentially, and some cyclohexanone (CHONE), in the gas-phase conversion of cyclohexanol. On the other hand, $NaMgPO_4$ produces CHONE selectively under the same reaction conditions. © 1995 Academic Press, Inc.

INTRODUCTION

The oxidation of primary and secondary alcohols to carbonyl compounds is of great interest for industrial and organic synthesis, and has so far been addressed by using both homogeneous and heterogeneous catalysis (1). The conversion of cyclohexanol to cyclohexanone (2, 3) has received much attention lately as ketone is the starting material for manufacturing nylon. Secondary alcohols provide good ketone yields. On the other hand, the oxidation of primary alcohols must be stopped at the aldehyde in order to avoid the formation of carboxylic acids, which demands strict control of the reaction conditions. There are a number of available procedures for selectively converting a primary or secondary alcohol into the corresponding aldehyde or ketone, respectively, by using gaseous reactants and metal oxides such as MgO (4), ZnO (5, 6), FeO (7, 8), Cr_2O_3, and NiO–CuO (10) as catalysts.

Some orthophosphates, including $AlPO_4$ (11–14), $BiPO_4$ (15–17), BPO_4 (18), $FePO_4$ (19), Li_3PO_4 (20), and several others (12), have also been used in organic synthesis. In fact, most of these compounds are active in the gas-phase dehydration of alcohols (21) over the temperature range 523–773 K (the actual temperature depends on the particular orthophosphate). In addition, some [e.g., hydroxyapatite, $Ca_{10}(OH)_2(PO_4)_6$ (22), $Zn_3(PO_4)_2$ (23), and calcium nickel phosphate (24)] exhibit a dehydrogenating ability in the conversion of secondary alcohols to ketones. For example, hydroxyapatite at a surface P/Ca ratio above 0.63 leads to the dehydration product exclusively. Below such a ratio, both the dehydrogenation and the dehydration product are obtained. The selectivity of zinc orthophosphate depends on the temperature at which it is heated in the preparation procedure (573–923 K). Thus, the solids obtained at the lower temperatures provide higher yields of butenes (the dehydration products) in the conversion of 2-butanol; on the other hand, the solids heated at temperatures close to 923 K yield 2-butanone (the dehydrogenation product) preferentially.

The dehydration of an alcohol usually competes with its dehydrogenation; the proportion of each type of product depends on the particular catalyst and reaction conditions used. The catalyst selectivity is dictated by its acid–base and redox properties (25–28), which are acquired during the synthetic process. The addition of various doping agents such as nitrates and carbonates (29–32) to SiO_2, Al_2O_3, Cr_2O_3, and MgO alters the activity and selectivity of these catalysts in various organic processes.

This paper reports on the activity- and selectivity-enhancing effect of the addition of sodium carbonate during the synthesis of a magnesium orthophosphate. The modified solid yields cyclohexanone highly selectively from cyclohexanol.

[1] To whom correspondence should be addressed.

0021-9517/95 $12.00
Copyright © 1995 by Academic Press, Inc.
All rights of reproduction in any form reserved.

EXPERIMENTAL

Catalyst Synthesis

A 3 *N* NaOH solution was added dropwise to an aqueous solution containing 232 g of $MgCl_2 \cdot 6H_2O$ and 115 g of Na_2HPO_4 up to pH 9. The precipitate thus formed,

$$3\,MgCl_2 + 2\,Na_2HPO_4 \rightarrow Mg_3(PO_4)_2 + 4\,NaCl + 2\,HCl, \quad [1]$$

was allowed to stand and was then filtered and air-dried in order to obtain a solid that was called MgP. Twenty-five grams of the solid was then suspended in 200 ml of water at 343 K and 100 ml of a saturated Na_2CO_3 solution was added dropwise. The solid obtained after 24 h of standing, NaMgP, was filtered and air-dried. Finally, each solid was calcined stepwise by using the following temperature programme: 1 h at 473 K, 1 h at 573 K, 1 h at 673 K, and 1 h at 773 K.

After calcination at 773 K, solid NaMgP was washed with water several times until no chloride was detected ($AgNO_3$ reaction) in the washings. Once dry, the solid was subjected to the same temperature programme as the previous solid. The final product was called $NaMgP_W$.

Solid MgO_S was prepared by using a procedure similar to that for NaMgP. Thus, to an aqueous solution containing 232 g of $MgCl_2 \cdot 6H_2O$, 3 *N* NaOH was added dropwise up to pH 9. A portion of the precipitate formed (25 g) was suspended in 100 ml of an Na_2CO_3 solution for 24 h. After filtering and drying, the solid was subjected to the above-described calcination programme.

Catalysts MgP_C (Aldrich, ref. 34, 470-2) and MgO_C (Probus, ref. 3225) were commercially available solids of formula $Mg_3(PO_4)_2 \cdot xH_2O$ and $Mg(OH)_2$, respectively. Both were subjected to the same calcination procedure as the synthesized solids.

All solids were sifted through 200–250 mesh.

X-Ray Diffraction Analysis

X-ray diffraction (XRD) patterns were recorded on a Siemens D 500 diffractometer using CuK_α radiation. Scans were performed over the 2θ range from 7 to 50.

TGA and MS Measurements

Thermogravimetric curves were recorded on a Cahn 2000 electrobalance in a nitrogen atmosphere by heating from 298 to 1123 K at a rate of 10 K min^{-1}. Samples were used untreated.

Mass spectra were obtained by fitting a VG-Sensorlab spectrometer to the outlet of quartz reactor that was placed in a heating oven. Samples were calcined at 973 K in an Ar stream at 50 ml min^{-1}; the heating rate used was 10 K min^{-1}. The amount of CO_2 released was determined from a preliminary calibration.

SEM Measurements

Scanning electron micrographs were obtained by using gold-coated samples on a Jeol JSM-5400 instrument equipped with a Link ISI analyser and a Pentafet detector (Oxford) for energy dispersive X-ray analysis (EDAX).

XPS Measurements

XPS experiments were carried out on a Leybold-Heraeus LHS-10 spectrometer using a constant pass energy of 50 eV, and MgK_α radiation for excitation ($h\nu$ = 1253.6 eV). XPS recordings were all run at a final pressure of 10^{-9} Torr.

IR Spectra

Diffuse reflectance infrared spectra for the synthesized solids were recorded from 400 to 6000 cm^{-1} on a Bomen MB-100 FTIR spectrophotometer. Samples were prepared by mixing 0.14 g of powdered solid with KBr (the blank) in a 15:85 ratio. All samples were preheated at 573 K in order to remove any water.

Chemical and Textural Properties of the Catalysts

The specific surface area of the synthesized solids was determined by using the BET method on a Micromeritics ASAP 200 analyser.

Acid, basic, and oxidizing sites were quantified from the retention isotherms for three different titrants (cyclohexylamine, phenol, and phenothiazine, respectively), dissolved in cyclohexane. The amount of titrant retained by each solid was measured spectrophotometrically (λ_{max} = 226, 271.6, and 238 nm for cyclohexylamine, phenol, and phenothiazine, respectively). By using the Langmuir equation, the amount of titrant adsorbed in monolayer form, X_m, was obtained as a measure of the concentration of acid and basic sites (33).

Reactor

Reactions were carried out in a tubular glass reactor of 20 mm i.d. that was fed at the top with cyclohexanol by means of a Sage 35 propulsion pump the flow-rate of which was controlled via a nitrogen flow-meter. The reactor was loaded with 4 g of catalyst, over which was placed 5 g of glass beads acting as a vaporizing layer. The temperature was controlled via an externally wrapped heating wire that covered the height of both the catalytic bed and the vaporizer, and was connected to a temperature control. Evolved gases from the reactor were passed through a condenser and onto a collector that allowed liquids to be withdrawn at different times.

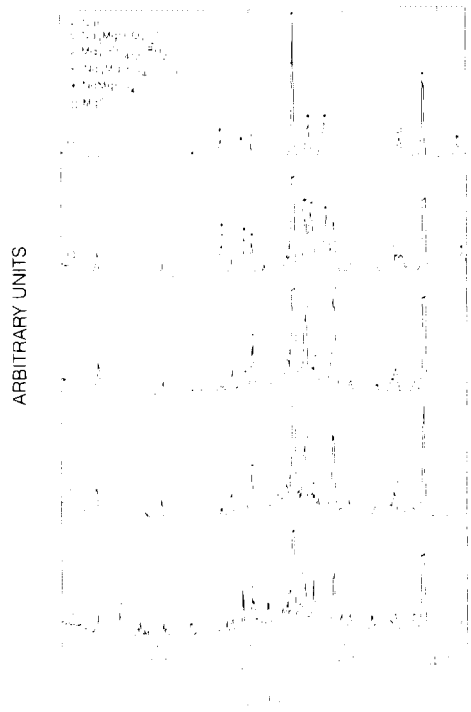

FIG. 1. XRD patterns for solid NaMgP obtained at different calcination temperatures: r.t. (a), 473 K (b), 573 K (c), 673 K (d), and 773 K (e).

No diffusion control mechanism was detected (34), nor was any of the reactor elements found to contribute to the catalytic effect under the working conditions (feed rate = 0.15–60 ml min^{-1}, T = 473–823 K; N_2 flow rate = 100 ml min^{-1}; amount of catalyst = 2–5 g) in preliminary blank runs.

Collected samples were analysed by gas chromatography on a 2 m × 1/8 in I.D. column packed with Carbowax over Chromosorb P-10% CW 20 M, using a linear temperature programme (from 333 to 423 K at 30 K min^{-1}). The products obtained were identified by comparison with standards and their structures confirmed by mass spectrometry.

RESULTS AND DISCUSSION

XRD Results

Figure 1 shows the XRD patterns obtained for catalyst NaMgP calcined at different temperatures. The patterns were recorded for samples obtained at various calcination stages. At room temperature, this solid was found to be a complex mixture of species that were characterized from 2θ ASTM values. The mixture included $Mg_3(PO_4)_2 \cdot 8H_2O$ (2θ = 13.4), NaCl (2θ = 27.2, 31.7, 45.4), $Na_3Mg(CO_3)_2Cl$-like chlorocarbonates (2θ = 11.1, 18.0, 27.5, 31.2, 33.0, 33.9, 36.0, 37.7, 42.4) and, possibly, carbonates, the diffraction patterns for which were quite ill-defined. These species are consistent with the synthetic procedure used and undergo various transformations during calcination. Thus, $Mg_3(PO_4)_2 \cdot 8H_2O$ may be dehydrated below 473 K and lose some crystallinity. Kanazawa *et al.* (35) detected this transformation at 403 K and low pressure, and at 423–463 K and atmospheric pressure. On the other hand, the chlorocarbonate species occur in the solid up to 673 K. Also, phosphocarbonates of formula $Na_3Mg(CO_3)PO_4$ (2θ = 24.3, 26.6, 33.6) are present in the solid between 573 and 673 K. Above the latter temperature, they start to decompose and disappear altogether by the time 773 K is reached. A correlation between the diffraction bands for the solids calcined at 673 and 773 K suggests the decomposition of the phosphocarbonates to $NaMgPO_4$ (2θ = 24.1, 26.4, 33.5, 35.1, 49.0) and Na_2CO_3. On the other hand, the chlorocarbonates are seemingly unstable above 673 K, where they decompose to NaCl, Na_2CO_3, and $MgCO_3$. While the carbonates resulting from the phosphocarbonates and chlorocarbonates cannot be identified from the diffraction patterns, their presence has been irrefutably confirmed by FTIR spectroscopy as shown below.

Hydroxycarbonates of formula $Mg_4(OH)_2(CO_3)_3 \cdot 3H_2O$ were detected in solid MgO_S prior to calcination. On calcining at 773 K, the hydroxycarbonates decomposed to periclase MgO (2θ = 40.7, 62.1, 72.2, 78.2), CO_2, and H_2O. The most typical diffraction line for periclase MgO (2θ = 40.7) was very well-defined in the pattern for solid NaMgP calcined at 773 K. Other, weaker diffraction lines did not appear on the chart, but were indeed detected. This magnesium oxide may have been formed by a similar procedure to that for the hydroxycarbonates, even though the species were not clearly detected in the intermediate solid calcination steps.

Washing NaMgP calcined at 773 K thoroughly (until any chloride was absent from the washings) resulted in the loss of most soluble species (NaCl and Na_2CO_3, mainly). The massive removal of Na^+ ions gave rise to structural alteration of the solid. Thus, the diffraction bands recorded after washing coincided with those for $Mg_3(PO_4)_2 \cdot 22H_2O$, which is the magnesium orthophosphate species obtained by some authors in an aqueous medium (36). Calcination of the washed solid ($NaMgP_W$) at 773 K turned it amorphous.

All other solids were characterized from their diffraction patterns at room temperature. Thus, MgP_C, MgP, and MgO_C were found to consist of $Mg_3(PO_4)_2 \cdot 8H_2O$, $Mg_3(PO_4)_2 \cdot 22H_2O$, and brucite, respectively. Solid MgO_S was a mixture of the hydroxycarbonate $Mg_4(OH)_2(CO_3)_3 \cdot 3H_2O$ (2θ = 9.7, 13.8, 15.3, 19.8, 21.2, 27.0, 30.9, 41.9), $Na_2Mg(CO_3)_2$ (2θ = 23.4, 32.8, 34.4, 36.2, 40.0, 43.6, 47.9, 60.4), and brucite (2θ = 18.7, 37.9, 50.9, 58.5). All these solids except MgO_C and MgO_S, characterized as periclase, became amorphous on calcination at 773 K.

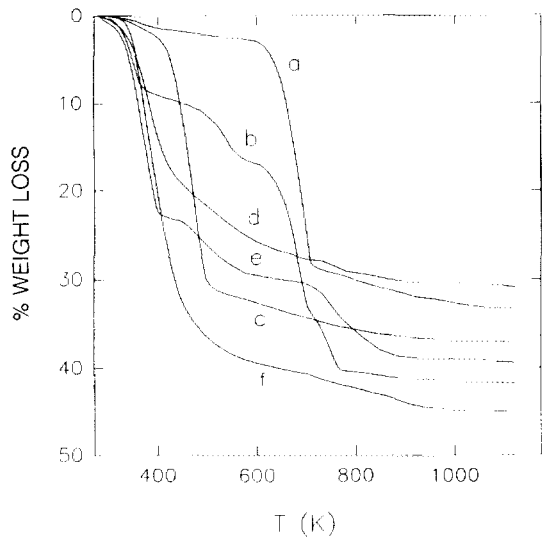

FIG. 2. TGA curves for the synthesized solids: MgO_C (a), MgO_S (b), MgP_C (c), MgP (d), NaMgP (e), and $NaMgP_W$ (f).

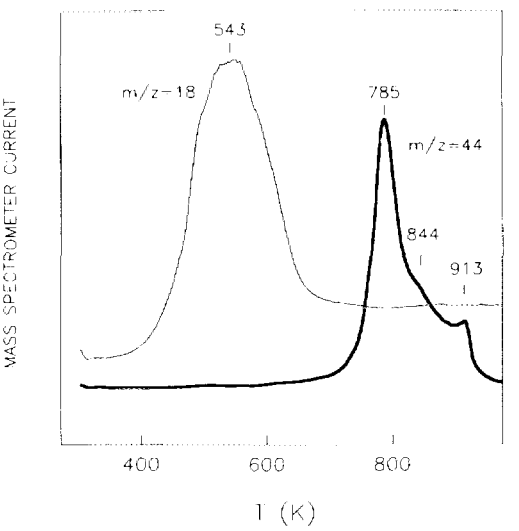

FIG. 3. Monitoring of the CO_2 and H_2O released in the calcination of solid NaMgP.

TGA Results

Figure 2 shows the TGA obtained for the different synthesized solids. All TGA curves were run at room temperature. Solids MgP and MgP_C underwent a substantial weight loss (31 and 37%, respectively) below 523 K. Several variably hydrated magnesium phosphates have been shown to experience a similar water loss (37). Solid MgO_C also lost much water (33%) over the temperature range 593–713 K. The conversion of $Mg(OH)_2$ into MgO takes place over the range 673–723 K (38) and the oxide can be rehydrated at room temperature (39). This process is accelerated by chloride impurities (40). The fact that the slopes of the TGA curves for solids MgO_C and MgO_S between 600–703 K are identical suggests that the former may also be involved in the conversion of brucite $Mg(OH)_2$ to periclase MgO at these temperatures.

The TGA curves for solids MgO_S and NaMgP, which were doped with sodium carbonate during their synthesis, are somehow special. In fact, they show two water losses at 523 and below 703 K, and a further weight loss above 703 K. Most halotropic forms of magnesium carbonate reportedly decompose above 823 K (41); however, the actual temperature may vary with the working conditions and nature of the sample. Thus, Leofanti *et al.* (42) found the presence of chloride ion to favour water and CO_2 removal at lower temperatures relative to some magnesium hydroxycarbonates. Also, Na_2CO_3 may be decomposed above 1023 K (43).

In order to characterize the gases released in the decomposition of the samples, the NaMgP solid was heated under the same conditions used to record the TGA curves (viz. an argon stream at 50 ml min^{-1} and a heating rate of 10 K min^{-1}). By fitting a mass spectrometric detector to the reactor outlet, two ions [m/z ($H_2O\cdot^+$) = 18 and m/z ($CO_2\cdot^+$) = 44] were monitored throughout the temperature range studied (Fig. 3). The weight losses observed below 673 K were assigned to water, the loss of which was maximal at 543 K. Some CO_2 was detected between 673 and 923 K. Obviously, the weight loss observed in this temperature range can be ascribed to the decomposition of the magnesium carbonates or magnesium hydroxycarbonates in solids NaMgP and MgO_S. Release of CO_2 was maximal at 785 K. A smaller CO_2 loss was detected from 843 to 913 K that was possibly due to the decomposition of minor halotropic forms of magnesium carbonate. The weight losses determined from the TGA curves (8.6%) and MS (9.0%) over the range 678–923 K were quite consistent. The temperature at which all the solids were calcined (773 ± 10 K) makes decomposition of the Na_2CO_3 present unlikely.

SEM Results

Figure 4 shows the micrographs obtained for the synthesized solids, calcined at 773 K. As can be seen, the appearance of the commercially available magnesium orthophosphate (Fig. 4a) and that synthesized in this work (Fig. 4b) is rather different. On the other hand, catalyst MgP_C is more homogenous as regards particle size (particles possess an elongated shape and an uneven profile). Catalyst MgP contains large particles that are covered with spongy glomeruli. An EDAX analysis showed the two phases to be identical.

The appearance of the solid obtained by including Na_2CO_3 in the synthetic procedure (solid NaMgP, Fig. 4c)

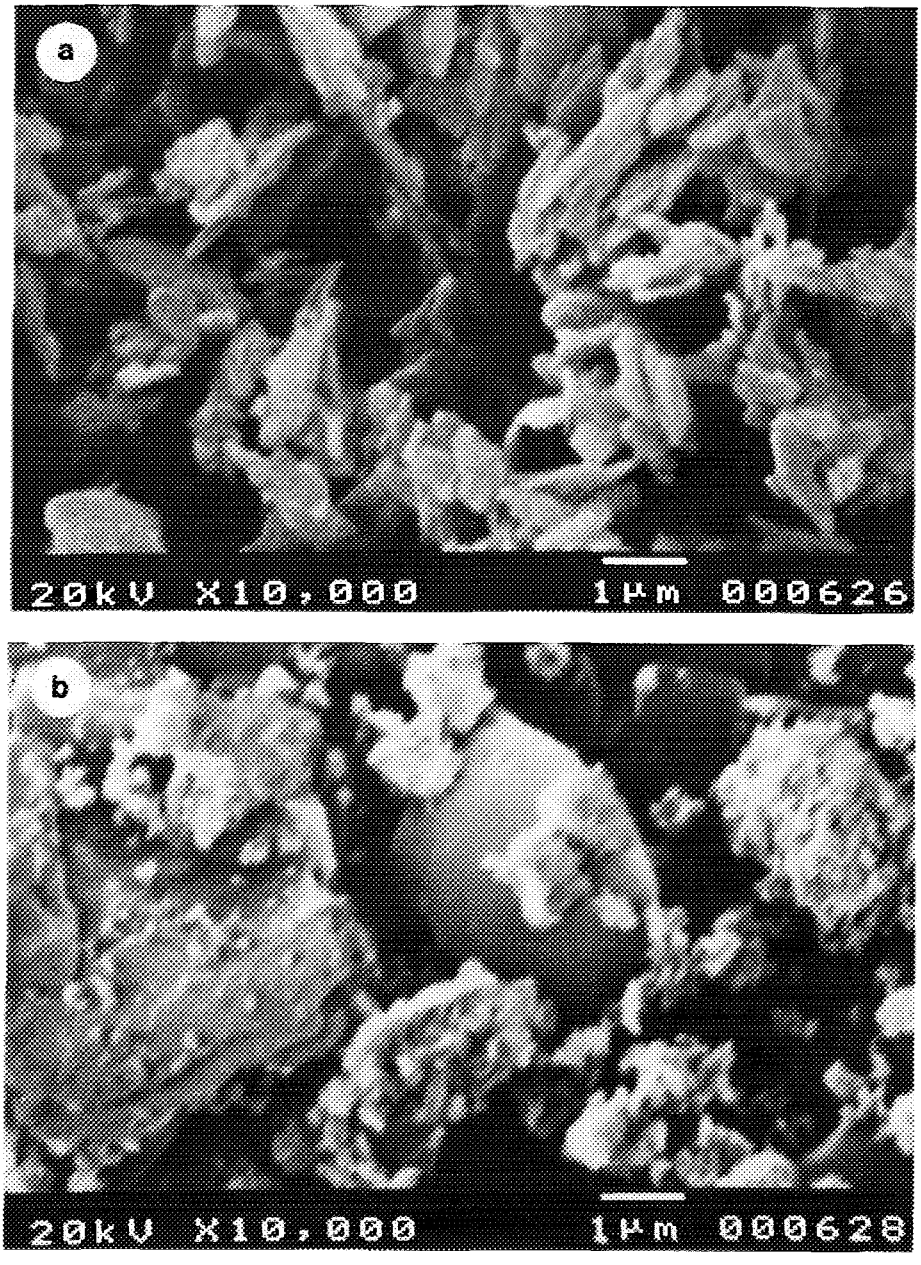

FIG. 4. Scanning electron micrographs of the synthesized solids: MgP_C (a), MgP (b), NaMgP (c), $NaMgP_W$ (d), MgO_C (e), and MgO_S (f).

was completely different. It consisted of randomly oriented laminar units impregnated with spongy forms. An EDAX analysis showed such forms to be NaCl. Washing the solid thoroughly with water gave rise to a major morphological change (solid $NaMgP_W$, Fig. 4d). Thus, the particle surface was spongy, so the surface area was larger. Washing removed soluble species (particularly NaCl) and induced significant morphological and surface changes.

Figures 4e and 4f compare the commercially available magnesium oxide (MgO_C) and that prepared in this work (MgO_S)—in the absence of Na_2HPO_4. While MgO_C is a highly spongy solid with a large surface area, the synthesized oxide consists of many distorted spherical particles of a highly uniform size ($\varnothing$ = 0.5 μm) that associate to form larger agglomerates. The results obtained from the SEM data are highly correlated with the specific surface areas given in Table 3.

XPS and EDAX Results

Table 1 gives the percent surface elemental composition of the solids and Table 2 lists the atomic ratios determined

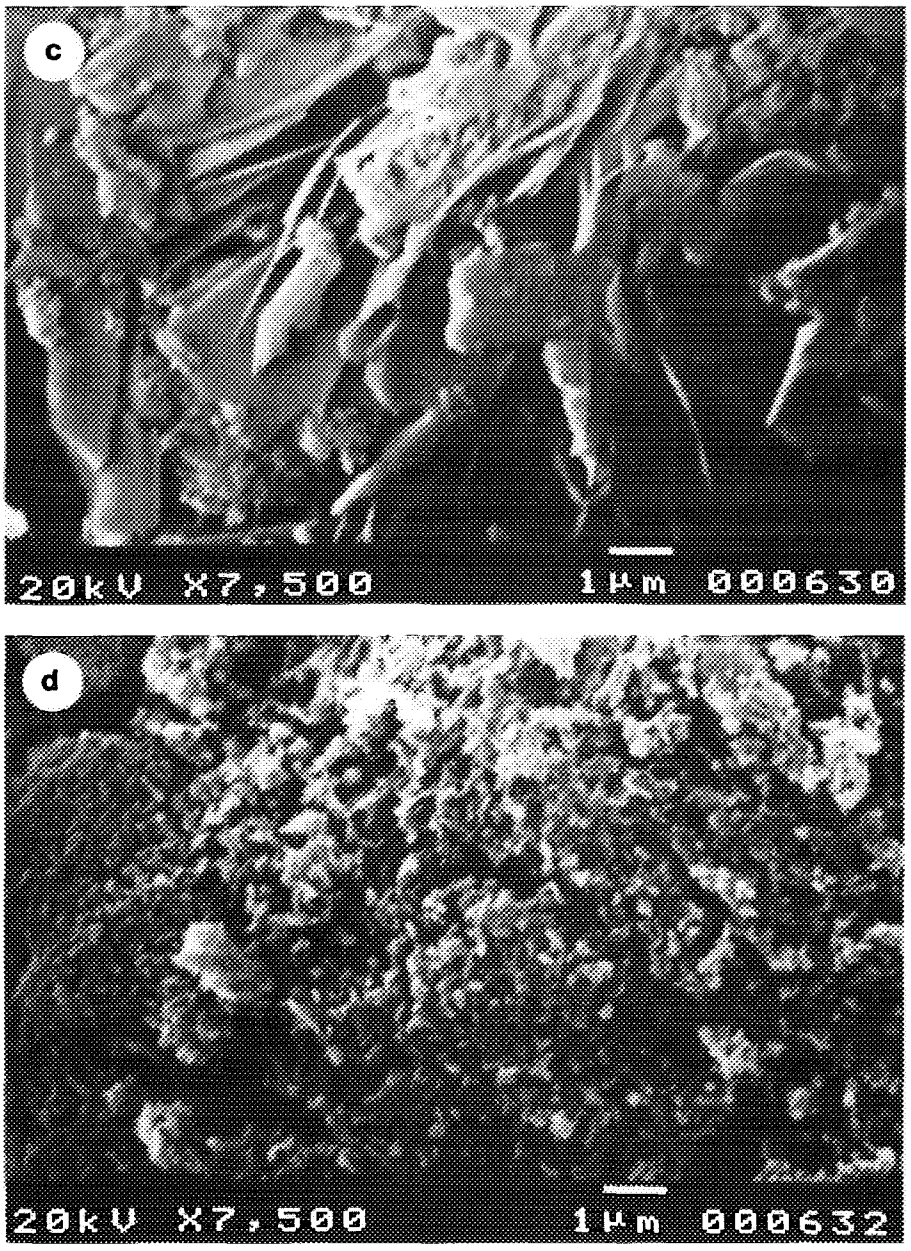

FIG. 4—*Continued*

by EDAX and XPS. Even though the depth of the layer accessed in an EDAX analysis depends on the density of the sample concerned and the voltage used—which was constant for all of our samples—it usually ranges from 50 to 500 Å, so the information provided by this technique corresponds to a deeper zone than that explored by the XPS technique (3–4 nm).

As a rule, the XPS data suggest that the solid surface was the portion where the atomic composition was most widely variable; in fact, the surface of the synthesized solids may have retained anions and cations present in the reaction medium. Hence, the surface analyses may have provided atomic compositions that were inconsistent with the expected stoichiometries. In fact, the composition in the deeper layers of a crystallite was closer to the theoretical stoichiometry.

The O/Mg ratios obtained for solids MgO_S and MgO_C are consistent with brucite-like magnesium hydroxides [$Mg(OH)_2$]. Synthetic MgO_S was found to contain Na^+, Cl^-, and nongraphite C from surface carbon residues.

The Na/Cl ratios provided by EDAX and XPS were all higher than unity. This may have been the result of the

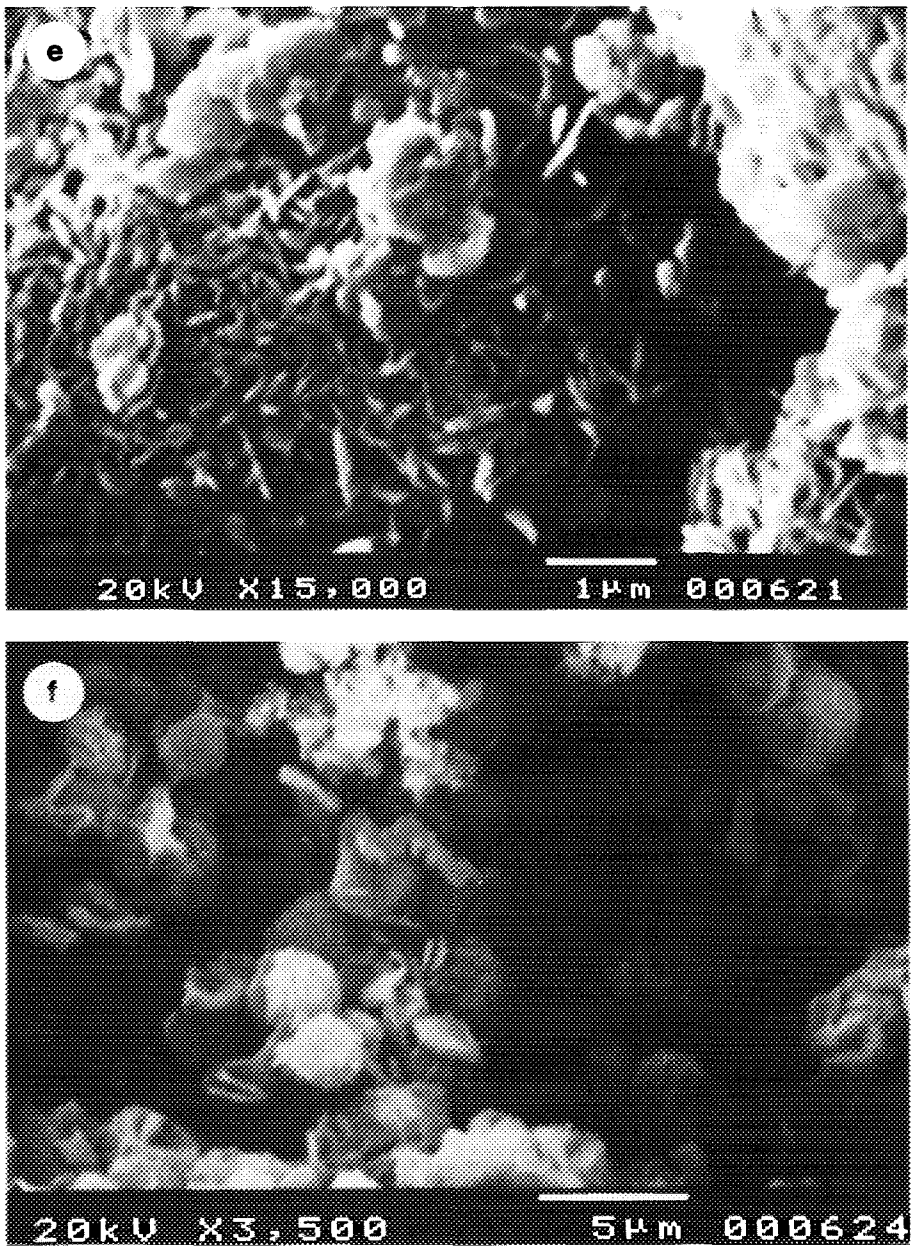

FIG. 4—*Continued*

overall amount of Na being made up of the contributions of NaCl species formed by reaction [1], and Na_2CO_3. All the solids whose synthesis included addition of Na_2CO_3 (MgO_S and NaMgP) exhibited an Na/Cl ratio greater than 2.

A comparison of the results for solids MgP_C and MgP reveals that, while their O/Mg ratio is slightly higher than the stoichiometric ratio (O/Mg = 2.66), that for the synthetic solid is somewhat higher than the ratio for its commercially available counterpart.

Those solids to which sodium carbonate was added (NaMgP and MgO_S) were found to contain much surface carbon and oxygen.

The addition of Na_2CO_3 during the catalyst synthesis gave rise to the presence of carbonates and other species (possibly MgO) on the solid surface, which in turn increased its oxygen surface content. The magnesium oxide may have originated from the decomposition of basic magnesium carbonates to CO_2 and MgO above 703 K because Na_2CO_3 is stable at the calcination temperature used. The resulting increase in the amount of surface Mg may have lowered the P/Mg ratio to 0.52.

TABLE 1

Percent Elemental Composition (at.%) of the Elements Present in the Solids Calcined at 773 K as Determined by XPS and EDAX

Catalyst	Element	XPS[a]	EDAX
MgO_C			
	Mg	34.31 (1*s*, 1304.7 eV)	33.23
	O	65.69 (1*s*, 531.4 eV)	66.77
MgO_S			
	Mg	26.10 (1*s*, 1304.7 eV)	34.59
	O	56.60 (1*s*, 531.6 eV)	59.20
	Na	5.20 (1*s*, 1072.2 eV)	4.32
	Cl	2.30 (2*p*, 199.2 eV)	1.89
	C	9.60 (1*s*, 290.4 eV)	—
MgP_C			
	Mg	20.95 (1*s*, 1305.5 eV)	22.32
	P	13.90 (2*p*, 133.5 eV)	13.60
	O	64.95 (1*s*, 531.6 eV)	64.08
MgP			
	Mg	18.23 (1*s*, 1305.0 eV)	15.96
	P	13.75 (2*p*, 133.6 eV)	8.20
	O	60.99 (1*s*, 531.6 eV)	55.76
	Na	4.48 (1*s*, 1072.5 eV)	11.78
	Cl	2.35 (2*p*, 199.2 eV)	8.30
NaMgP			
	Mg	14.10 (1*s*, 1304.7 eV)	12.57
	P	7.40 (2*p*, 133.2 eV)	2.73
	O	58.10 (1*s*, 531.4 eV)	55.77
	Na	8.60 (1*s*, 1072.1 eV)	19.86
	Cl	2.30 (2*p*, 199.2 eV)	9.07
	C	9.20 (1*s*, 290.4 eV)	—
$NaMgP_W$			
	Mg	22.80 (1*s*, 1304.8 eV)	21.23
	P	11.79 (2*p*, 133.3 eV)	8.90
	O	62.97 (1*s*, 531.3 eV)	66.07
	Na	2.34 (1*s*, 1072.1 eV)	2.58
	Cl	—	1.22

[a] XPS binding energies are given in brackets.

TABLE 3

Chemical and Textural Properties of the Solids Calcined at 773 K

Catalyst	S_{spec} ($m^2\ g^{-1}$)	Acidity[a,d] (10^6 mol g^{-1})	Basicity[b,d] (10^6 mol g^{-1})	Oxid. sites[c,d] (10^8 mol g^{-1})
MgP_C	5	24	11	—
MgP	15	61	20	11
NaMgP	10	12	5	11
$NaMgP_W$	21	49	44	18
MgO_S	24	<1	51	306
MgO_C	105	33	147	2115

[a] Vs cyclohexylamine.
[b] Vs phenol.
[c] Vs phenothiazine.
[d] The values reported are multiplied by 10^6 or 10^8.

Washing the catalyst dissolved a substantial amount of soluble substances on the surface. In fact, the amount of NaCl decreased and surface carbonate disappeared altogether on washing; however, the P/Mg ratio remained unchanged, so washing seemingly removed no magnesium-containing species. As a result, the residual P and Mg atoms brought the O/P and O/Mg ratios closer to the theoretical stoichiometries. Washing enriched the solid surface with oxygen relative to the bulk medium, possibly via a simultaneous hydroxylation process, which is consistent with the increased acidity and basicity values given in Table 3. The thoroughness of the washing procedure is clearly apparent from the complete absence of surface Cl^- ions after it—only a very small amount of NaCl was detected by EDAX.

DRIFT Spectra

Figure 5 shows the DRIFT spectra for the calcined solids at 773 K. The doublet at 1532 and 1432 cm^{-1} for NaMgP

TABLE 2

Atomic Ratios Obtained from the XPS and EDAX Data Given in Table 1

	XPS ratio			EDAX ratio			Theoretical ratio		
Catalyst	O/Mg	P/Mg	O/P	O/Mg	P/Mg	O/P	O/Mg	P/Mg	O/P
MgO_C	1.90	—	—	2.00	—	—	2.00[a]	—	—
MgO_S	2.16	—	—	1.71	—	—	2.00[a]	—	—
MgP_C	3.10	0.66	4.60	2.87	0.58	4.71	2.66	0.66	4.00
MgP	3.30	0.75	4.43	3.49	0.51	6.80	2.66	0.66	4.00
NaMgP	4.10	0.52	7.85	4.43	0.2	20.4	4.00[b]	1.00	4.00
$NaMgP_W$	4.10	0.52	5.34	3.11	0.41	7.40	2.66	0.66	4.00

[a] For $Mg(OH)_2$ as the predominant species on surface.
[b] For $NaMgPO_4$ as the predominant species.

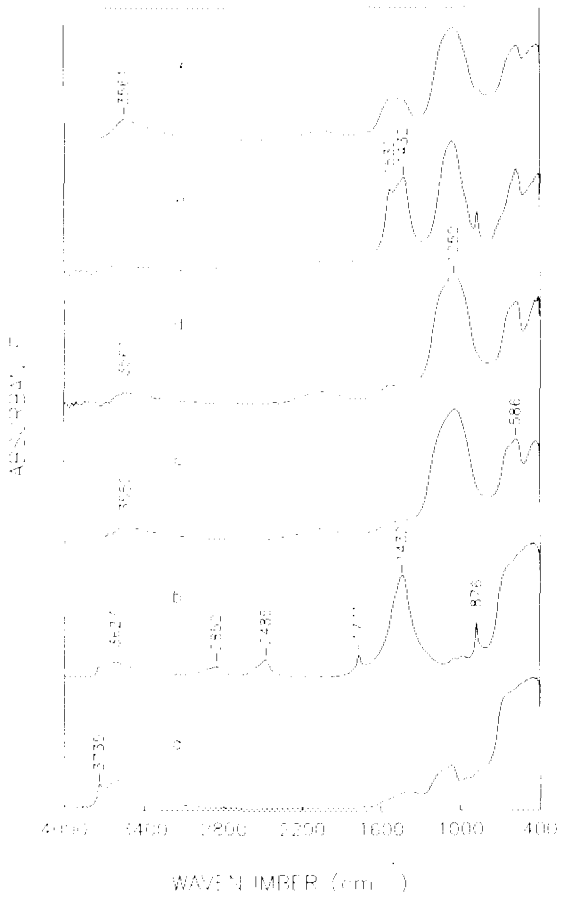

FIG. 5. DRIFT spectra for the solids calcined at 773 K: MgO_C (a), MgO_S (b), MgP_C (c), MgP (d), NaMgP (e), and $NaMgP_W$ (f).

suggests the presence of carbonates. The latter band is also exhibited by MgO_S, which also included sodium carbonate in its preparation; however, the peak at 1532 cm^{-1} is rather ill-defined. Both solids exhibit a characteristic band at 876 cm^{-1} that is occasionally used to distinguish carbonates from phosphates (44, 45). This band is absent from the spectra for MgP and MgP_C, the synthesis of which involved no sodium carbonate, even though they include the above-mentioned doublet—much weaker, however—probably resulting from small amounts of carbonate being formed on calcination in air. The calcination programme used (773 K, 1 h) probably did not remove magnesium carbonate altogether, which, however, cannot be ascertained from the DRIFT spectra. Phillipp *et al.* (46) and several other authors (47–49) assign a doublet at 1526 and 1419 cm^{-1} to symmetric, asymmetric, and stretching vibrations of surface monodentate carbonates formed by adsorption of CO_2 and MgO.

Inorganic phosphates of general formula $M_3^{\text{I}}PO_4^{3-}$ give a strong band in the region 1050–1000 cm^{-1} (50). There is also evidence of a second absorption band at 980 cm^{-1} (51, 52). The band observed between 1000 and 1100 cm^{-1} in the phosphates studied is rather broad, so it does not allow one to distinguish between phosphate varieties. Solid MgP_C exhibits a similar band at 1035 cm^{-1}.

Washing solid $NaMgP_W$ has a twofold effect. On the one hand, it considerably decreases the bands at 876, 1786, 2530, and 2905 cm^{-1} through removal of most water-soluble sodium carbonate; on the other, it increases the bands between 3000 and 4000 cm^{-1}, which is consistent with increased hydroxylation of the solid. The hydroxyl groups concerned (3561 cm^{-1}) seemingly come from P–OH bonds (14), which are very week in solid NaMgP. The band at 3735 cm^{-1} and those between 3670 and 3500 cm^{-1} for solid MgO_S have been ascribed to various Mg–OH groups (39). Thus, Anderson *et al.* (53) assign the band at 3735 cm^{-1} to hydroxyl groups bound to surface magnesium atoms and the frequency group between 3650 and 3550 cm^{-1} to hydroxyls bound to the second magnesium atom layer. Coluccia *et al.* (54) also ascribe this band group to hydroxyls bonded to magnesium atoms located on the crystallite sides, which facilitates massive interaction with other, neighbouring hydroxyls; they assign the band at 3735 cm^{-1} to hydroxyl groups at crystallite edges and corners. None of these bands are observed in the spectrum of $NaMgP_W$. Rather, the solid is very similar to MgP and MgP_C in this spectral region (3000–4000 cm^{-1}).

Figure 6 compares the FTIR spectrum for solid MgO_S with that for a commercially available magnesium hydroxycarbonate (Panreac, ref. 151395); both were recorded at room temperature by using the pellet technique. As can be seen, the two spectra are identical, except for the abundant Mg–OH groups (3700 cm^{-1}) in MgO_S that are absent from

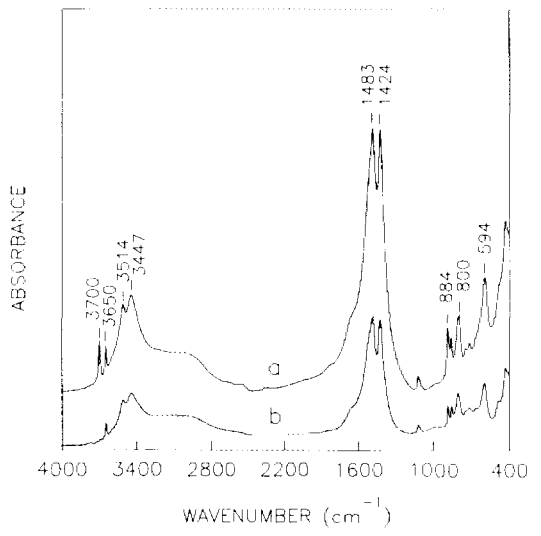

FIG. 6. FTIR spectra for a commercially available magnesium hydroxycarbonate (b) and solid MgO_S (a), both uncalcined.

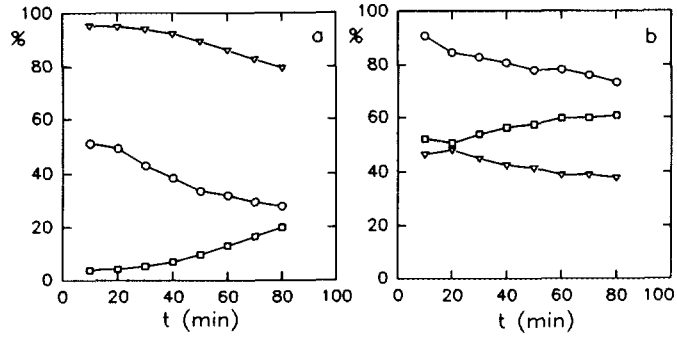

FIG. 7. Variation of the overall conversion (○) and selectivity towards cyclohexene (CHE) (▽) and cyclohexanone (CHONE) (□) of catalyst MgP with the reaction time at 673 K (a) and 773 K (b).

the commercially available hydroxycarbonate, probably as a result of the presence of $Mg(OH)_2$ in the synthesized solid. Both solids produce periclase MgO on calcination, as checked by X-ray diffraction spectroscopy.

Textural and Surface Acid–Base Properties

Table 3 summarizes the textural properties, as well as the acid, basic, and oxidizing site concentration of the catalysts studied.

As a rule, the synthesized solids had a small surface area. However, catalyst MgP, prepared in this work, had a larger surface and larger surface acid and basic site populations than the commercially available magnesium orthophosphate. A comparison of the results for catalysts MgP, NaMgP, and $NaMgP_W$ clearly reveals the effect of adding sodium carbonate and subsequently washing the solid. In fact, the addition of Na_2CO_3 to the reaction medium gives rise to several species that are deposited on the solid surface, thereby decreasing its surface area and its acid and basic site populations. Washing solid $NaMgP_W$ with water dissolves soluble species and consequently increases the solid surface area and its populations of acid and basic sites through the formation of new surface hydroxyls. The magnesium oxide prepared in this way contains no cyclohexylamine-titratable acidity, but includes a large population of basic sites—not so large as that of commercially available MgO_C, however.

Catalytic Activity

Figures 7a and 7b show the conversion and selectivity towards CHE and CHONE obtained in the dehydration–dehydrogenation of cyclohexanol at 673 and 773 K for solid MgP. While the overall conversion increased with increasing reaction temperature, the selectivity towards CHE and CHONE varied markedly with the temperature. Thus, CHE was preferentially obtained at 673 K, while CHONE was predominantly obtained at 773 K. These results are consistent with the occurrence of a different type of site for the dehydration and dehydrogenation of the alcohol. Some authors associate dehydration with acid surface sites (55) and dehydrogenation with basic surface sites (56, 57). Several zeolites are believed to use both types of sites to convert methanol (58), but there is no conclusive evidence in this respect. As a rule, active sites involved in the dehydrogenation process act at higher temperatures than do active sites effecting dehydration (59); both processes may thus compete over an intervening temperature range. Which catalyst properties govern its action on the conversion of CHOL into CHE and CHONE remains to be clarified (60).

TABLE 4

Activity and Selectivity of the Catalyst Calcined at 773 K in the Conversion of Cyclohexanol, $T_{reaction}$ = 773 K

Catalyst	X_{TOTAL} (mol %)	S_{CHONE}	S_{CHE}	$r_a \cdot 10^4$
MgO_C	99.0	0.53	0.08	6.4
MgO_S	74.4	0.98	0.01	21.0
MgP_C	99.5	0.00	0.96	134.9
MgP	73.2	0.61	0.38	33.1
NaMgP	64.0	0.99	0.01	43.4
$NaMgP_W$	98.9	0.13	0.85	31.9

Note. Reactions conditions: W/F (feed mol $^{-1}$ h g_{cat}) = 14.75; N_2 flow-rate, 100 ml min $^{-1}$; amount of catalyst, 4 g; $t_{reaction}$ = 80 min. S_{CHONE} (selectivity towards CHONE), CHONE conversion/overall conversion; S_{CHE} (selectivity towards CHE), CHE conversion/overall conversion. r_a, specific catalytic activity (mol h $^{-1}$ m $^{-2}$).

Table 4 compares the activity of the solids in the gas-phase dehydration–dehydrogenation of cyclohexanol. Solids MgO_C and MgO_S exhibit the typical activity and selectivity of magnesium oxide (61) in alcohol oxidations. Solid MgO_S is highly selective towards CHONE, whereas MgO_C is not. In addition, the latter gives a high proportion of condensation, isomerization and polymerization byproducts as the likely result of its large populations of acid and oxidizing sites relative to the other solids. A comparison of the results for the magnesium orthophosphates (MgP_C and MgP) reveals that the commercially available solid produces CHE selectively (plus less than 4% metylcyclopentene isomers), whereas the synthesized solid yields CHONE predominantly. Solid NaMgP, obtained by addition of Na_2CO_3 to MgP, produces CHONE selectively. Washing their water brings its activity and selectivity closer to those of magnesium orthophosphates. However, commercially available sodium carbonate gives no reaction with cyclohexanol under the same reaction conditions used with the previous solids.

All these activity and selectivity results are highly correlated with the structural, compositional and surface hydra-

tion changes revealed by the different characterization techniques used. However, further tests (e.g., D/H exchange, selective poisoning) are required in order to gather more precise information of the active surface of the catalysts.

CONCLUSIONS

The addition of Na_2CO_3 to freshly made $Mg_3(PO_4)_2 \cdot 22H_2O$, followed by digestion at 343 K, leads to $NaMgPO_4$ preferentially on calcination at 773 K. Some intermediate species including magnesium carbonates, chlorocarbonates, and phosphocarbonates are formed in the intervening steps that decompose at the calcination temperature. The surface of the final solid contains MgO, Na_2CO_3, and NaCl, which alter the activity and selectivity of the resulting catalyst. Freshly prepared magnesium orthophosphate yields CHE and CHONE from gas-phase CHOL, whereas solid $NaMgPO_4$, obtained by addition of Na_2CO_3, yields CHONE selectively. Removing soluble species by washing the solid gives rise to $Mg_3(PO_4)_2 \cdot 22H_2O$, which, after calcination, yields CHE highly selectively. The high complexity of the solid surface hindered its characterization, which is currently in progress. The role and amount of each species present on the solid surface must also be elucidated in order to correctly correlate the activity and selectivity of the synthesized solids.

ACKNOWLEDGMENTS

The authors express their gratitude to the Spanish DGICyT for funding this work in the framework of Project PB92-0816. F. J. Romero is also grateful to the Consejería de Educación y Ciencia de la Junta de Andalucía for award of a grant. Finally, the staff at the Servicio de Espectroscopía de Fotoelectrones of the Faculty of Chemistry of the University of Seville is gratefully acknowledged for recording the XPS/ESCA spectra analysed in this work.

REFERENCES

1. Hudlicky, M., "Oxidations in Organic Chemistry," ACS Monograph 186. Am. Chem. Soc., Washington, DC, 1990.
2. Dobrovolszky, M., Tetenyi, P., and Paal, Z., *J. Catal.* **74,** 31 (1982).
3. Pridman, V. Z., Bedina, L. N., and Petrov, I. Y., *Kinet. Katal.* **29,** 621 (1988). [English translation 535, 1988]
4. Stobbe, D. E., Buren, F. R., Groenendijk, P. E., Dillen, A. J., and Geus, J. W., *J. Mater. Chem.* **1,** 539 (1991).
5. Tsuchida, T., and Kitajima, S., *Chem. Lett.*, 1769 (1990).
6. Hino, M., and Arata, K., *Chem. Lett.*, 1737 (1990).
7. Mazanec, T. J., *J. Catal.* **98,** 115 (1986).
8. Sreerama, M., Patnaik, P., Sidneswaran, P., and Jayamani, M., *J. Catal.* **109,** 298 (1988).
9. Nondek, L., Mihajlova, D., Andreev, A., Palazov, A., Kraus, M., and Shopov, D., *J. Catal.* **40,** 46 (1975).
10. Paal, Z., Peter, A., and Tetenyi, P., *React. Kinet. Catal. Lett.* **1,** 121 (1974).
11. Campelo, J. M., García, A., Luna, D., Marinas, J. M., *J. Catal.* **111,** 106 (1988).
12. Moffat, J. B., *in* "Topics in Phosphorous Chemistry" (M. Grayson and E. J. Griffith, Eds.), Vol. 10, p. 285. Wiley, New York, 1980.
13. Campelo, J. M., García, A., Luna, D., Marinas, J. M., *J. Catal.* **102,** 299 (1986).
14. Peri, J. B., *Disc. Faraday Soc.* **52,** 55 (1971).
15. Sakamoto, T., Egashira, M., and Seiyama, T., *J. Catal.* **16,** 407 (1970).
16. Seiyama, T., Egashira, M., Sakamoto, T., and Aso, I., *J. Catal.* **24,** 76 (1972).
17. Ruwet, M., Ceckiewicz, P., and Delmon, B., *Ind. Eng. Chem. Res.* **26,** 10 (1987).
18. Moffat, J. B., and Neeleman, J. F., *J. Catal.* **31,** 274 (1973).
19. Giorgini, M., Bartolozzi, M., F. Morelli, and Di Manno, A., *Ann. Chim. (Rome)* **65,** 29 (1975).
20. Coudurier, M., Mathieu, M. V., Prettre, M., Imelik, B., and Degeorges, M. E., *Bull. Soc. Chim. Fr.*, 1821 (1968).
21. Thomke, K., and Noller, H., *in* Proceedings, 5th International Congress on Catalysis, Pal Beach (J. W. Hightower, Ed.) Vol. 2, p. 84. North Holland, Amsterdam, 1973.
22. Kibby, C. L., and Hall, W. K., *J. Catal.* **31,** 65 (1973); **29,** 144 (1973).
23. Tada, A., Itoh, H., Kawasaki, J. M., and Nara, J., *Chem. Lett.*, 517 (1975).
24. Ruwet, M., Berteau, P., and Ceckinwicz, S., *Bull. Soc. Chim. Belg.* **96,** 281 (1987).
25. Tanabe, K., Misono, M., Ono, I., and Hattori, N., *Stud. Surf. Sci. Catal.*, **51** (1989).
26. Winterbottom, J. M. *in* "Catalysis," vol. 4, p. 141. Royal Chem. Soc., London, 1981.
27. Ai, M., *J. Catal.* **49,** 305 (1977).
28. Ouqour, A., Coudurier, G., and Vedrine, J. C., *J. Chem. Soc. Faraday Trans.* **89,** 3151 (1993).
29. Perrichon, V., and Durupty, M. C., *Appl. Catal.* **42,** 217 (1988).
30. Ganesan, K., and Pillai, C. N., *J. Catal.* **119,** 8 (1989).
31. Ramana, D. V., and Pillai, C. N., *Can. J. Chem.* **47,** 3705 (1969).
32. Montagne, X., Durand, C., and Mabilon, G., *in* "Catalysis by Acids and Bases" (B. Imelik, C., Naccache, G. Coudurier, Y. Ben Taarit, and J. C. Vedrine, Eds.), p. 33. Elsevier, Amsterdam, 1985.
33. Aramendía, M. A., Borau, V., Jiménez, C., Marinas, J. M., and Rodero, F., *Colloids Surf.* **12,** 227 (1984).
34. Koros, R. M., and Novak, E. J., *Chem. Eng. Sci.* **22,** 470 (1967).
35. Kanazawa, T., Umegaki, T., and Wasai, E., *Chem. Lett.* 817 (1974).
36. Bakaev, A. Y., Dzis'ko, U. A., Karakchiev, L. G., Moroz, E. M., Kustova, G. N., and Tsikova, L. T., *Kinet. Katal.* **5,** Vol. 15, 1275 (1974).
37. Kanazawa, T., Umegaki, T., and Kawazoe, H., *in* "Proceedings, 1st International Congress on Phosphorus Compounds," p. 107. Rabat, 1977.
38. Beck, C. W., *Am. Mineral.* **35,** 985 (1950).
39. Morrow, B. A., *in* "Studies in Surface Science and Catalysis" (J. L. G. Fierro, Ed.), Vol. **57A,** p. A202. Elsevier, New York, 1990.
40. Holt, T. E., Logan, A. D., Chakraborti, S., and Datye, A. K., *Appl. Catal.* **34,** 199 (1987).
41. Webb, T. L., and Krüger, J. E., *in* "Differential Thermal Analysis" (R. C. MacKenzie, Ed.), p. 312. Academic Press, London, 1970.
42. Leofanti, G., Solari, M., Tauszik, G. R., Garbassi, F., Galvagno, S., and Schwank, J., *Appl. Catal.* **3,** 131 (1982).
43. "Handbook of Chemistry and Physics," 68th ed. CRC Press, Boca Raton, FL, 1987.
44. Pobeguin, T., and Lecomte, J., *Compl. Rend. Acad. Sci. (Paris)* **236,** 1544 (1953).

45. Pobeguin, T., *J. Phys. Radium* **15,** 410 (1954).
46. Phillipp, R., Omata, K., Aoki, A., and Fujimoto, K., *J. Catal.* **134,** 422 (1992).
47. Zhang, G., and Hattori, H., *in* "Acid-Base Catalysis" (K. Tanabe, H. Hattori, T. Yamaguchi, and T. Tanaka, Eds.), p. 475. Kodansha, Tokyo, 1989.
48. Little, L. H., "Infrared Spectra of Adsorbed Species," pp. 76–77. Academic Press, London, 1966.
49. Lercher, J. A., Colombier, C., and Noller, H., *J. Chem. Soc. Faraday Trans* **180,** 949 (1984).
50. Bellamy, L. J., "The Infrared Spectra of Complex Molecules," p. 363. Chapman & Hall, London, 1975.
51. Bergmann, E. D., Littauer, U. Z., Pinchas, S., *J. Chem. Soc.*, 847 (1952).
52. Nakamoto, K., "Infrared and Raman Spectra of Inorganic and Coordination Compounds," 4th ed., p. 139. Wiley, New York, 1986.
53. Anderson, P. J., Horlock, R. F., and Oliver, J. F., *J. Chem. Soc. Faraday Trans.* **61,** 2754 (1965).
54. Coluccia, S., Lavagnino, S., and Marchese, L., *Mater. Chem. Phys.* **18,** 445 (1988).
55. Figueras-Rocca, F., Mourgues, L., and Trambouze, Y., *J. Catal.* **14,** 107 (1969).
56. Matsumura, Y., Hashimoto, K., and Yoshida, S., *J. Catal.* **117,** 135 (1989).
57. Thomke, K., *Z. Phys. Chem. N. F.* **106,** 225 (1977).
58. Lin, L., Tobias, R. G., McLaughlin, K., and Anthony, R. G., "Gas and Alcohols to Chemicals" (R. G. Herman, Ed.), p. 323. Plenum, New York, 1984.
59. Yashima, T., Suzuki, H., and Hara, N., *J. Catal.* **33,** 486 (1974).
60. Rao, P. K., Sivaraj, C., Srinivasa, S. T., and Rao, V. N., "Catalysis of Organic Reactions" (W. E. Pascoe, Ed.), p. 194. Dekker, New York, 1992.
61. Szabo, Z. G., Jover, B., and Ohmacht, R., *J. Catal.* **39,** 225 (1975).